arXiv:1002.0843v1 [nlin.CD] 3 Feb 2010

A Markov Chain Approximation of a Segment Description of Chaos

Alexander Labovsky and Y. Charles Li

Abstract. We test a Markov chain approximation to the segment description (Li, 2007) of chaos (and turbulence) on a tent map, the Minea system, the Hénon map, and the Lorenz system. For the tent map, we compute the probability transition matrix of the Markov chain on the segments for segment time length (iterations) $T = 1, 2, 3, 100$. The matrix has $1, 2, 4$ tents corresponding to $T = 1, 2, 3$; and is almost uniform for $T = 100$. As $T \to +\infty$, our conjecture is that the matrix will approach a uniform matrix (i.e. every entry is the same). For the simple fixed point attractor in the Minea system, the Reynolds average performs excellently and better than the maximal probability Markov chain and segment linking. But for the strange attractors in the Hénon map, and the Lorenz system, the Reynolds average performs very poorly and worse than the maximal probability Markov chain and segment linking.

Contents

1. Markov Chain Approximation 2
2. Ulam Approximation 2
3. Asymptotic Cycles 3
4. Transition Matrix 3
5. Different Types of Orbits 3
6. Minea System 4
7. Hénon Map 5
8. Lorenz System 5
9. Conclusion and Discussion 5
References 6

1991 *Mathematics Subject Classification.* Primary 37, 76; Secondary 34, 35.

Key words and phrases. Markov chain, Ulam approximation, segment description, chaos, Lorenz system.

Labovsky's current address: Florida State University, Department of Scientific Computing, Tallahassee, FL 32306-4120.

©2006 (copyright holder)

1. Markov Chain Approximation

In [**3**], we showed that any orbit inside an attractor (chaotic or turbulent attractors are the most interesting ones) can be uniformly approximated on the infinite time interval $t \in [0, \infty)$ by an infinite sequence of segments out of a finite number of segments. The attractor (or its attracting neighborhood) is partitioned into N small neighborhoods $\{A_n\}_{n=1,2,\cdots,N}$. Each neighborhood A_n is attached with an orbit segment s_n over a fixed time interval $t \in [0, T]$. Denote by F^t the evolution operator. The flow tube $\cup_{t\in[0,T]} F^t(A_n)$ is approximated by the segment s_n. If $F^T(A_n) \cap A_m \neq \emptyset$, then the flow tube $\cup_{t\in[T,2T]} F^t(F^T(A_n) \cap A_m)$ is approximated by the segment s_m. This process can be continued to $t \to \infty$. If we re-distribute the Lebesgue measure of $F^T(A_n) \cap A_m$ uniformly on A_m (i.e. we assume the points in $F^T(A_n) \cap A_m$ as random points with uniform probability distribution in A_m), then we obtain a Markov chain approximation. When A_n's are small and the attractor has good mixing properties, we expect this Markov chain approximation to perform very well. The key element for this Markov chain approximation is the transition matrix [**2**], [**1**]

$$\Lambda = (\rho_{ij}) \ , \tag{1}$$

where

$$\rho_{ij} = \frac{\mu(F^T(A_j) \cap A_i)}{\mu(F^T(A_j))} \ ,$$

and μ is the Lebesgue measure. We can simply label A_n and s_n by the letter n. Then our Markov chain is defined by the transition matrix Λ acting on N letters $\{1, 2, \cdots, N\}$.

2. Ulam Approximation

The Transfer Operator (Perron-Frobenius Operator) is defined as,

$$\nu_{n+1}(A) = \nu_n(F^{-T}(A)) = \sum_{j=1}^{N} \nu_n(F^{-T}(A) \cap A_j) \ , \tag{2}$$

where ν_n's are measures. The Ulam approximation of the transfer operator is defined as,

$$\nu_{n+1}(A) = \sum_{j=1}^{N} \frac{\mu(F^{-T}(A) \cap A_j)}{\mu(A_j)} \nu_n(A_j) \ , \tag{3}$$

where μ is the Lebesgue measure. If we re-distribute $\nu_n(F^{-T}(A) \cap A_j)$ uniformly on A_j (i.e. we assume the points in $F^T(A) \cap A_j$ as random points with uniform probability distribution in A_j), then we obtain the Ulam approximation by

$$\nu_n(F^{-T}(A) \cap A_j) \sim \frac{\mu(F^{-T}(A) \cap A_j)}{\mu(A_j)} \nu_n(A_j) \ .$$

The transition matrix of the Ulam approximation is

$$P = (\sigma_{ij}) \ , \tag{4}$$

where

$$\sigma_{ij} = \frac{\mu(F^{-T}(A_i) \cap A_j)}{\mu(A_j)} \ .$$

If F^T is $1-1$ and we replace the partition $\{A_i\}$ by $\{F^T(A_i)\}$, then

$$\sigma_{ij} = \frac{\mu(A_i \cap F^T(A_j))}{\mu(F^T(A_j))} = \rho_{ij} \ .$$

3. Asymptotic Cycles

Using the segments $\{s_n\}_{n=1,2,\cdots,N}$, one can identify certain pseudo-orbits (called segment linking orbits) and the associated sequence of A_n's:

$$\cdots s_{n_{-2}} s_{n_{-1}} s_{n_0} s_{n_1} s_{n_2} \cdots$$
$$\cdots A_{n_{-2}} A_{n_{-1}} A_{n_0} A_{n_1} A_{n_2} \cdots$$

where s_{n_j} attaches to A_{n_j} and the end point of s_{n_j} belongs to $A_{n_{j+1}}$ (recall also that the starting point of s_{n_j} belongs to A_{n_j}). Since there are only finite s_n's; as $n_j \to +\infty$, some s_{n_j} has to repeat itself, then all the segments after it repeat themselves too. Thus all these pseudo-orbits are always asymptotic to cycles:

$$\cdots\cdots s_{n_{j_1}} \cdots s_{n_{j_k}} s_{n_{j_1}} \cdots s_{n_{j_k}} \cdots$$

where k can be 1 in which case the asymptotic cycle is a "fixed point".

4. Transition Matrix

We shall compute the transition matrix for the tent map:

$$x_{n+1} = f(x_n), \ x_n \in [0,1];$$

where

$$f(x_n) = \frac{x_n}{a} \ (x_n < a), \ f(x_n) = \frac{x_n - 1}{a-1} \ (x_n \geq a);$$

and a is a parameter $a \in (0,1)$. We choose $a = 1/3$. We break the interval $[0,1]$ into 20 subintervals. Take 100 initial conditions in each subinterval. For each initial condition x_0 in the i-th subinterval, we compute x_T as the T-iteration starting from x_0. If x_T belongs to j-th subinterval, we increase the (j,i)-th entry of the transition matrix by $\frac{1}{100}$. Initially all the entries of the transition matrix are set to 0. Since the iterated map f^T has 2^{T-1} tents, the transition matrix also resembles this pattern. Our conjecture is that when $T \to +\infty$, the transition matrix approaches a uniform matrix with every entry being $1/20$. See Figure 1 for an illustration.

5. Different Types of Orbits

We shall compute several types of orbits:

(1) **The true orbit**. It is computed by Runge-Kutta method for differential equations, and by iterations for maps; for a time interval $t \in [0, T^*]$.

(2) **The segment orbit**. First we cut the total time interval $[0, T^*]$ into subintervals of length T. The interested region in the phase space, where the attractor lives is partitioned into N small neighborhood $\{A_n\}_{n=1,2,\cdots,N}$ (usually squares or cubes). If at time $t = jT$, the true orbit lands in some A_n, then $(j+1)$-th segment will be the one attached to A_n (usually this segment is computed with the initial condition at the center of the square or cube for a time length of T). For $j = 0, 1, 2, \cdots$; all the segments together form the segment orbit. It is a uniform approximation of the true orbit for all positive time.

(3) **The segment linking orbit**. If the initial condition of the true orbit lands in some A_n, then the first segment will be the one attached to A_n. If the first segment ends in some A_m, then the second segment will be the one attached to A_m. By repeating this process, we generate the segment linking orbit. As discussed in Section 3, the segment linking orbit is asymptotic to some cycle. The segment orbit uniformly approximates a particular orbit in the basin of attraction, while the segment linking orbit only uses the initial condition of the true orbit, and is not a uniform approximation of the true orbit. In reality, the segment orbit is difficult to obtain without the full knowledge of the true orbit, while the segment linking orbit is trivial to obtain once all the segments attached to the A_n's are known.
(4) **The maximal probability Markov chain**. If the initial condition of the true orbit lands in some A_n, then the first segment will be the one attached to A_n. Then we test many random initial points in A_n, see where they land at time $t = T$, and we pick maximal probability partition element A_m. The second segment will be the one attached to A_m. Repeating the process, we generate the maximal probability Markov chain.
(5) **The Reynolds average orbit**. We pick initial conditions near the initial condition of the true orbit, compute the orbit corresponding to each initial condition, at each $t \geq 0$, we do an algebraic average of all the orbits, then we get the Reynolds average orbit.

Overall, the segment orbit is a uniform approximation of a particular orbit, while the segment linking orbit, the maximal probability Markov chain and the Reynolds average orbit are all aiming at certain average property of the attractor.

6. Minea System

Consider the Minea system

$$\begin{aligned} \frac{du_1}{dt} &= 1 - u_1 - \delta u_2^2 \ , \\ \frac{du_2}{dt} &= \delta u_1 u_2 - u_2 \ ; \end{aligned}$$

where $(u_1, u_2) \in (0,1) \times (0,1)$ and δ is a parameter. When $\delta > 1$, all the orbits converge to one point [**6**]. We choose $\delta = 5$ for our simulations here. The total simulation time $T^* = 10$, while the segment time $T = 1$ (i.e. 10 segments along each orbit). The interested region in the phase plane is $(u_1, u_2) \in (0,1) \times (0,1)$. We cut this unit square into 60×60 subsquares (i.e. the A_n's). The segment attached to each A_n starts from the center of A_n. The true orbit starts from the initial point $(\frac{1}{24}, 0.5 + \frac{1}{120})$. For the calculation of the maximal probability Markov chain, we test 1000 random initial points in A_n. For the calculation of the Reynolds average orbit, we pick 4 initial conditions within $\frac{1}{120}$ distance from the initial condition of the true orbit. The results are shown in Figure 2. As expected, the Reynolds average orbit is a better approximation of the true orbit than the other types of orbits.

7. Hénon Map

Consider the Hénon map

$$\begin{aligned} x_{n+1} &= y_n + 1 - 1.4x_n^2, \\ y_{n+1} &= 0.3x_n. \end{aligned}$$

The total simulation time $T^* = 1000$ (iterations), while the segment time $T = 250$ (i.e. 4 segments along each orbit). The interested region in the phase plane is $(x_n, y_n) \in (-2, 2) \times (-2, 2)$. We cut this square into 40×40 subsquares (i.e. the A_n's). The segments attached to each A_n starts from the center of A_n. The true orbit starts from the initial point $(0.631354477, 0.189406343)$. For the calculation of the maximal probability Markov chain, we test 1000 random initial points in A_n. For the calculation of the Reynolds average orbit, we pick 2 or 4 initial conditions within 10^{-6} distance from the initial condition of the true orbit. The results are shown in Figure 3. One thing is clear, that is, the Reynolds average orbits are definitely bad approximations to the true orbit, and bad descriptions of the strange attractor.

8. Lorenz System

Consider the Lorenz system

$$\begin{aligned} \frac{dx}{dt} &= a(y - x), \\ \frac{dy}{dt} &= x(b - 25z) - y, \\ \frac{dz}{dt} &= 25xy - cz, \end{aligned}$$

where we choose $a = 10$, $b = 28$, $c = 8/3$.

The total simulation time $T^* = 100$, while the segment time is either $T = 10$ (i.e. 10 segments along each orbit) or $T = 1$ (i.e. 100 segments along each orbit). The interested region in the phase space is $(x, y, z) \in (-0.8, 0.8) \times (-1, 1) \times (0, 2)$. We cut this region into $16 \times 16 \times 16$ subregions (i.e. the A_n's). The segments attached to each A_n starts from the center of A_n. The true orbit starts from the initial point $(0.1, 0, 0)$. For the calculation of the maximal probability Markov chain, we test 1000 random initial points in A_n. For the calculation of the Reynolds average orbit, we pick 2 or 4 initial conditions within 0.05 distance from the initial condition of the true orbit. The results are shown in Figures 4 and 5. Once again the Reynolds average orbits are definitely bad approximations to the true orbit, and bad descriptions of the strange attractor. Naturally as the number of the segments along an orbit increases, the segment linking orbit and the maximal probability Markov chain deviate further away from the true orbit.

9. Conclusion and Discussion

As discussed in details in [**3**] [**4**] [**5**], an effective description of turbulence means a solution to the problem of turbulence. An effective description of chaos is also very useful in applications of chaos theory.

It is dangerous to draw strong conclusion with limited numerical experiments. But it is clear from these numerical experiments here that the Reynolds average is a terrible description of strange attractors. The segment description has the potential

to generate useful descriptions of strange attractors. Both the segment linking and the Markov chain have the potential to generate useful characterizations on certain average properties of the strange attractors.

Traditionally the Reynolds average is based upon the setup of typical orbits being high frequency oscillations around a mean orbit. This is not the case inside a strange attractor. Therefore, one should not expect that the Reynolds average can be a good description on any sort of average property of the strange attractor. For the segment description, computing the segments can be costly if the partition is fine enough. Computing the segment orbit associated with a true orbit needs the full knowledge of the true orbit. So the potential of the segment description lies at the statistics of the segments rather than any individual segment orbit. Segment linking is a convenient way to start the study on the statistics of the segments. Markov chain is a first level study on the statistics of the segments. Practically it is very costly to generate the probability transition matrix for the Markov chain.

Finally what kind of average properties that a strange attractor may possess are not clear at all. If the strange attractor has ergodicity, then tracking one orbit is enough to get a good picture of the strange attractor. On the other hand, especially in higher dimensions, often the chaotic (turbulent) dynamics is transient. What kind of average properties that such transient dynamics may possess are even less clear.

References

[1] J. Ding, T.-Y. Li, A. Zhou, Finite approximations of Markov operators, *Journal of Computational and Applied Mathematics* **147** (2002), 137-152.

[2] J. Kemeny, J. Snell, *Finite Markov Chain*, D. Van Nostrand Company, Inc. Princeton, New Jersey, 1960.

[3] Y. Li, Segment description of turbulence, *Dynamics of PDE* **4, no.3** (2007), 283-291.

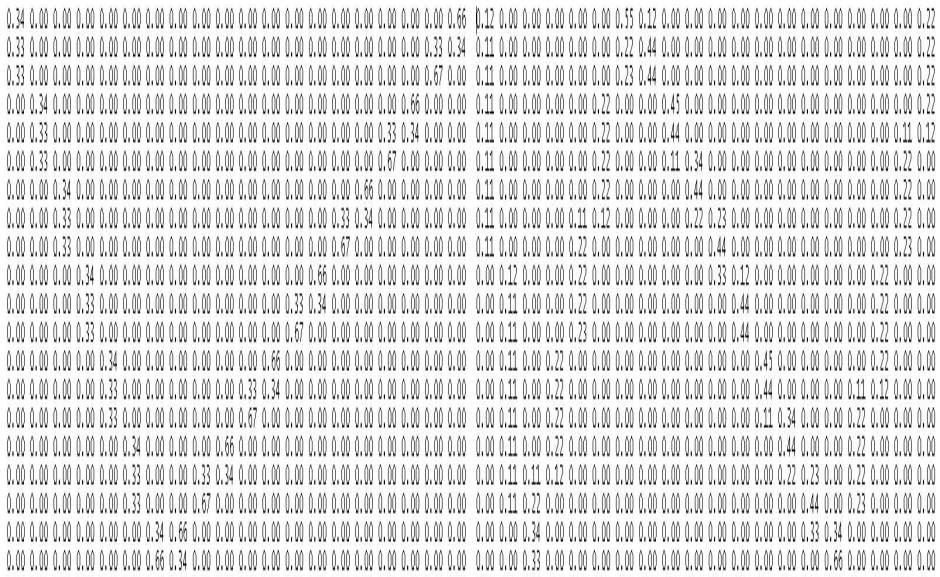
[4] Y. Li, Chaos in partial differential equations, Navier-Stokes equations and turbulence, *Proceedings of the 4th International Congress of Chinese Mathematicians*, (Hangzhou, December 17-22, 2007), vol. III, 110-122, Higher Education Press, Beijing, China

[5] Y. Li, On the true nature of turbulence, *The Mathematical Intelligencer* **29, no.1** (2007), 45-48.

[6] R. Temam, *Infinite-dimensional Dynamical Systems in Mechanics and Physics*, Springer-Verlag, 1988.

Department of Mathematics, University of Missouri, Columbia, MO 65211
E-mail address: alabovsky@sc.fsu.edu

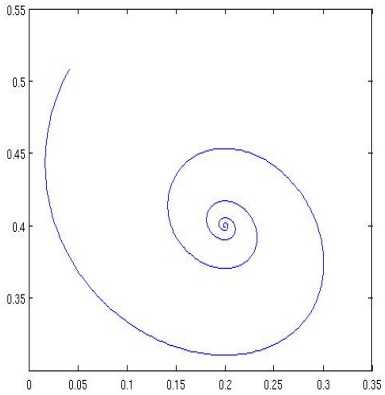
Department of Mathematics, University of Missouri, Columbia, MO 65211
E-mail address: liyan@missouri.edu



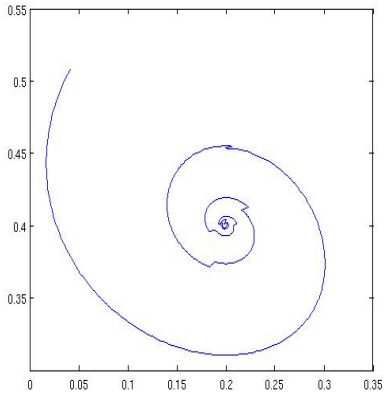
(a) $T = 1$ (b) $T = 2$

(c) $T = 3$ (d) $T = 100$

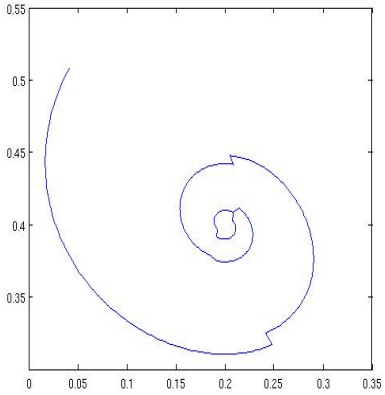
FIGURE 1. Transition matrices for the tent map



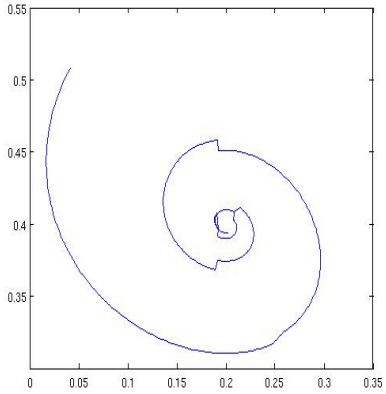
(a) true orbit



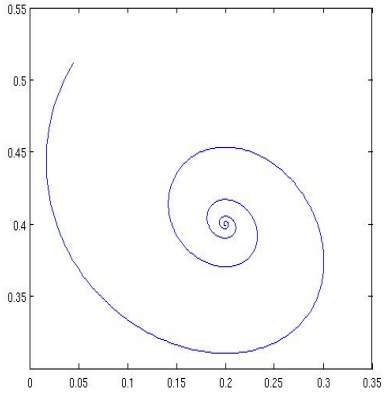
(b) segment orbit



(c) segment linking orbit

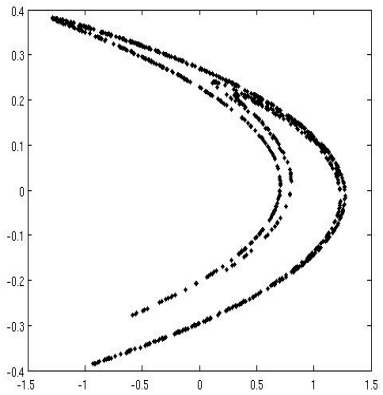


(d) maximal probability Markov chain

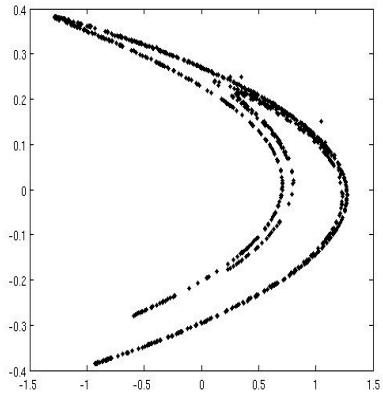


(e) Reynolds average orbit

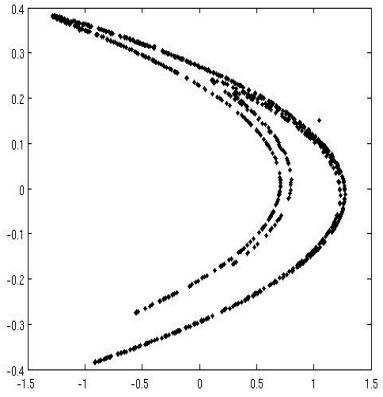
FIGURE 2. Different types of orbits for the Minea system.



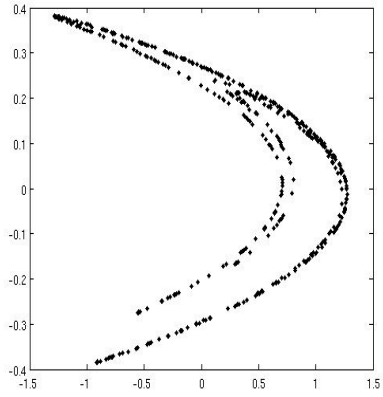
(a) true orbit



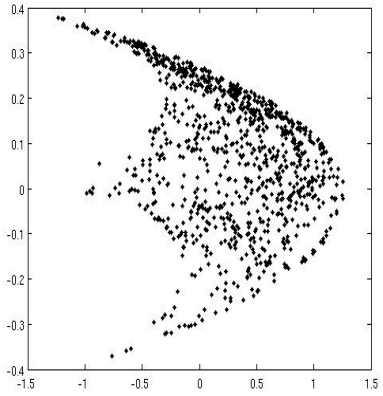
(b) segment orbit



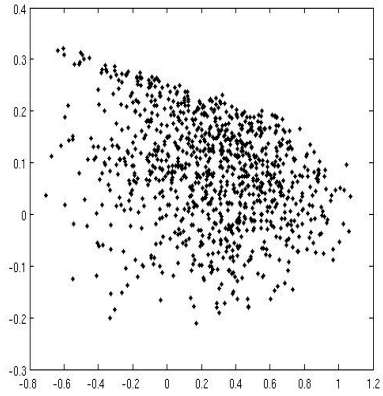
(c) segment linking orbit



(d) maximal probability Markov chain

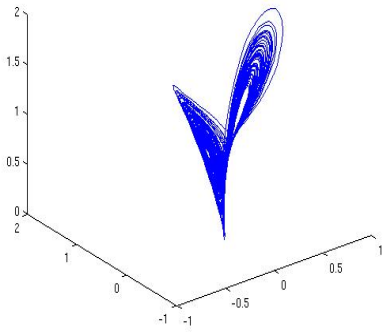


(e) Reynolds average orbit (of 2 orbits)

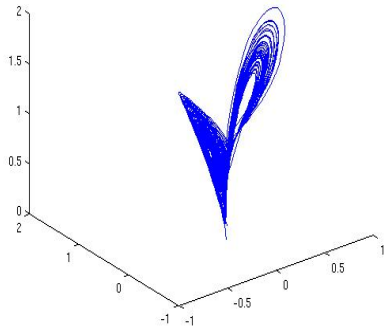


(f) Reynolds average orbit (of 4 orbits)

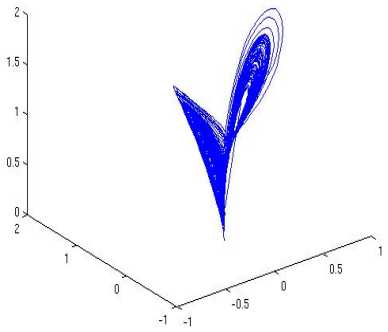
FIGURE 3. Different types of orbits for the Hénon map.



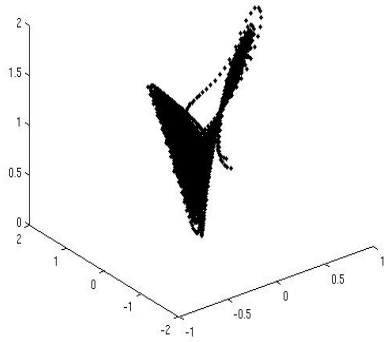
(a) true orbit



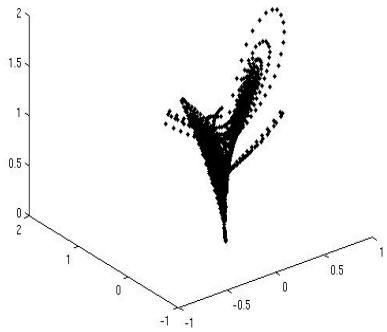
(b) segment orbit (10)



(c) segment orbit (100)

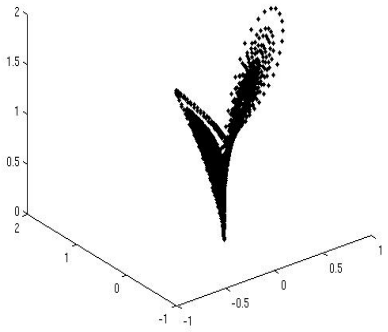


(d) segment linking orbit (10)

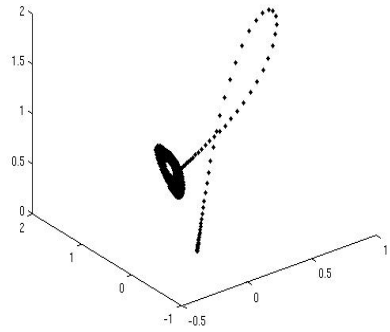


(e) segment linking orbit (100)

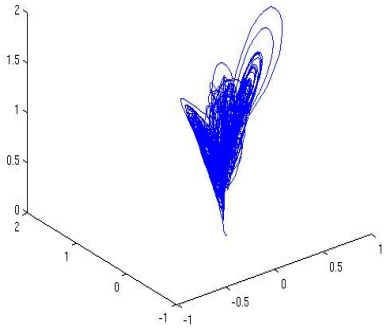
FIGURE 4. Different types of orbits for the Lorenz system (part 1).



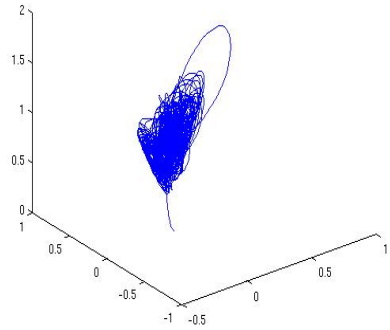
(a) maximal probability Markov chain (10)



(b) maximal probability Markov chain (100)



(c) Reynolds average orbit (of 2 orbits)



(d) Reynolds average orbit (of 4 orbits)

FIGURE 5. Different types of orbits for the Lorenz system (part 2).